Fizika Nizkikh Temperatur, 2007, v. 33, Nos. 6/7, p. 680–688

Electronically induced modification of thin layers on surfaces

U. Bauer, S. Neppl, D. Menzel[1], and P. Feulner

Physikdepartment E20, Technische Universität München, Germany
E-mail: feulner@tum.de

A. Shaporenko and M. Zharnikov

Angewandte Physikalische Chemie, Universität Heidelberg, Germany

Received November 7, 2006

Interactions of thermally and electronically stimulated reactions in thin layers on surfaces are investigated. For self-assembled monolayers, thermal activation promotes many processes primarily induced by electronic excitations. We demonstrate that the film temperature is an important parameter for steering these reactions towards different final products. Using chemisorbed water on Ru(001) as an example, we investigate how the products of an irradiation induced reaction catalyze thermally stimulated dissociation of water molecules.

PACS: **61.82.–d** Radiation effects on specific materials;
79.20.La Photon- and electron-stimulated desorption;
78.70.–g Interactions of particles and radiation with matter;
68.43.Vx Thermal desorption.

Keywords: thin layers, electronic excitations.

1. Introduction

Thermal excitations drive all kinds of reactions from diffusion to bond formation and bond breaking. The spectrum of excitation energies available to surmount activation barriers is a continuum described by the Boltzmann distribution. The energy range relevant for experimentally accessible reaction rates at a distinct temperature T is limited to less than $\sim 12\ kT$. The attempt frequencies of thermally stimulated reactions given by the ratios of partitioning functions of the initial and the transition states are large, typically 10^{13} s^{-1} and beyond; the initial and the transition states are commonly assumed to be in thermal equilibrium [1].

For reactions induced by electronic excitations, either by energetic particles or photons, the situation is completely different. Particularly photons from modern laser and synchrotron sources cover the entire valence and core electron excitation range. Specific electronically excited states at distinct sites in molecules and condensed matter can be selectively prepared by narrow bandwidth excitations, either such which are highly dissociative and break bonds, or such which turn an inert particle into a reactive one in order to make bonds. Apart from very few exceptions [2], electronically induced processes proceed far from equilibrium.

In practice, however, both scenarios may well be related. A good example is cryomicroscopy [3]. Energetic electrons in scanning or transmission electron microscopes, or photons in x-ray microscopes break bonds, but cryogenic conditions prevent structural changes mainly by hindering diffusion (see Ref. 3 and below). On the other hand, products of an electronically stimulated reaction may act as catalyst for further thermally activated process. In this contribution we report such interrelations of both reaction types for thin layers on surfaces. In the first section we focus on thermally stimulated processes promoting irradiation induced modifications of thin organic layers on metal and semiconductor surfaces. Using

[1] Also: Fritz-Haber-Institut der Max-Planck-Gesellschaft, Dept. CP, Berlin, Germany.

chemisorbed water on the Ru(001) surface as an example, we show in the second section how the products of an electronically stimulated process may catalyze a thermally induced conversion, thereby dramatically amplifying the effective conversion cross-section.

2. Examples and results

2.1. Thermal effects in beam induced modifications of self-assembled monolayers

Self-assembled monolayers (SAMs, Fig. 1) are well ordered arrangements of molecules consisting of headgroups with a specific affinity to the substrate, an aliphatic or aromatic backbone and an endgroup constituting the outer surface of the film (see Ref. 4 for further details).

The enormous potential of SAMs in many fields of technology is due to the flexibility in combining different structure elements (headgroup/backbone/endgroup) in order to suit the requirements of even very special applications (see [5] for an overview). SAMs serve as transfer agents in micro and nano printing techniques [5], as functional interfaces in bio sensors [5,6], as lubrication in micromechanics [5], corrosion protection [5], as ultrathin resists for lithography with ultimate resolution [5,7], but also as well defined model systems for organic layers on surfaces in fundamental research. Here we focus on the last point, using them for investigations of basic temperature effects on beam induced modifications. Many studies of irradiation effects in SAMs by electrons and to a lesser extent also by photons are reported in the literature, from which we cite three articles in which the reader can find most of the relevant references [8–10]. The majority of these previous reports are room temperature studies, thus neglecting any low-temperature effects. In order to close this gap, we have performed measurement between 50 and 300 K with synchrotron radiation (BESSY-II, U49-II-PGM-1) in the C1s and N1s excitation range for SAMs with aliphatic and aromatic backbones. Here we summarize the main results of these studies. For details of sample preparation, data acquisition or data evaluation the reader is referred to [11,12].

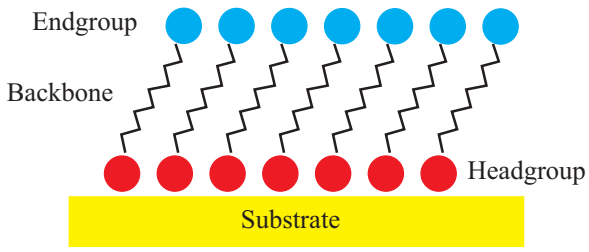

Fig. 1. Structure elements of self-assembled monolayers (see also [4,5]).

For the above temperature and energy range we find some electronically induced reactions which are nearly temperature independent, and others which strongly depend on the sample temperature. Nearly temperature independent radiation effects are those which do not involve transport of large fragments; abstraction of H atoms is the best example (see [10] for a description of the mechanism of electron stimulated H abstraction; although primary photons are applied in our study, secondary electrons with energies similar to those of [10] will stimulate the majority of abstraction processes even in our case, see below). Abstraction of H atoms leaves bond vacancies which recombine either by double bond formation (if at the same molecule) or by cross-linking (if at neighboring particles) [8]. The consequence of cross-linking will become obvious from results below, whereas double bond formation directly shows up in x-ray absorption spectroscopy (XAS).

Figure 2 shows XAS data for the C1s range from Au–S–$(CH_2)_{15}$–CH_3 SAMs. Apart from resonances at 288, 293 and 300 eV which are due to Rydberg, (C–H)-σ* and (C–C)-σ* excitations, respectively [8], an additional peak appears and grows at 285 eV for extended photon irradiation. This maximum has previously been assigned to double bond-derived [C1s]π* states formed as a result of radiation induced hydrogen abstraction [8,11]. Comparing data at 50 and 300 K, no significant temperature dependence is observed for the growth of this maximum as a function of photon exposure (Fig. 2 [11]). At 50 K it grows even slightly faster than at 300 K, due to rapid material loss at high temperatures, see below.

Compared with double bond formation after abstraction of hydrogen atoms, a completely different temperature dependence is obtained for the desorption of large

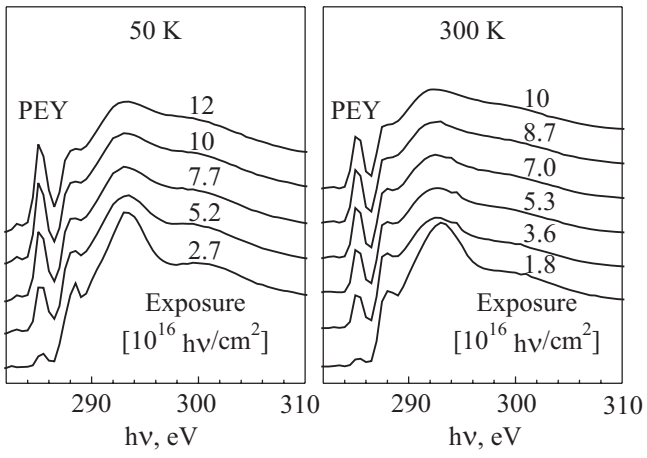

Fig. 2. C1s XAS for Au–S–$(CH_2)_{15}$–CH_3 SAMs, at 50 and 300 K (for A_z polarization, i.e., E-vector perpendicular to the surface normal, after [11]).

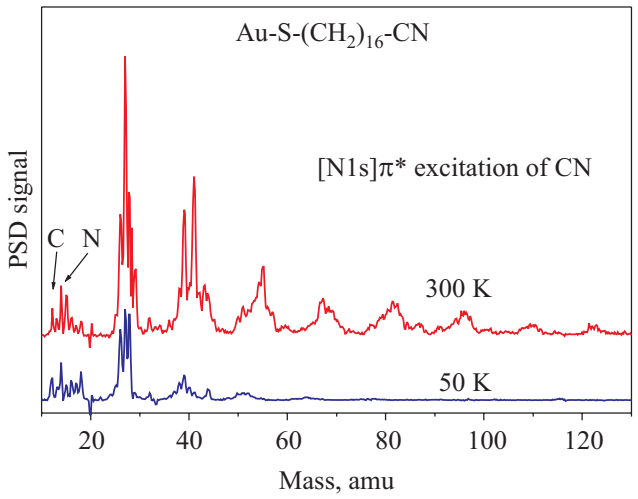

Fig. 3. PSD of neutrals by resonant [N1s]π* excitation from Au–S–$(CH_2)_{16}$–CN at 50 K and at 300 K (A_z-light).

hydrocarbon fragments by irradiation with soft x-ray photons. Figure 3 shows photon stimulated desorption (PSD) of neutral particles recorded with a mass spectrometer [13] from mercaptoheptadecanenitrile SAMs on Au.

At 300 K, PSD of large fragments is much more intense than at 50 K. We observe C_nH_x fragments up to $n = 9$ which is the upper limit of our mass spectrometer. At 50 K only fragments up to $n = 5$ are observable, all but those for $n = 1$ with much smaller amplitudes than at 300 K. Desorption of larger fragments requires their diffusive transport to the vacuum interface of the film which is hindered at cryogenic conditions by the lack of thermal stimulation. We believe that the suppression of electronically stimulated desorption of large fragments from organic films at low temperatures is a phenomenon of general validity. It has been observed not only for thiolate bonded SAMs on Au and Ag, but also for alkyls on silicon [11] and diamond [14], and for phosphonate bonded SAMs on silicon oxide [15].

We emphasize that the data of Fig. 3 have been obtained under π-resonant excitation of the CN endgroup, i.e., the primary excitation energy has been allocated to a specific bond of the molecule. Although this primary [N1s]π* state is not dissociative, population of highly repulsive final states is expected upon core decay. The products of these dissociation processes of the CN endgroup, namely C and N atoms, appear in the mass spectrum (Fig. 3). These site-specific signals which are due to direct photon induced bond breaking do not depend on temperature as expected. However, they are smaller than other desorption maxima even at 50 K. This indicates that the major part of the desorption signal from such layers is due to unspecific, not site selective excitations by secondary electrons, even for site selective primary excitations of states with large cross section such as the [N1s]π* resonance [16].

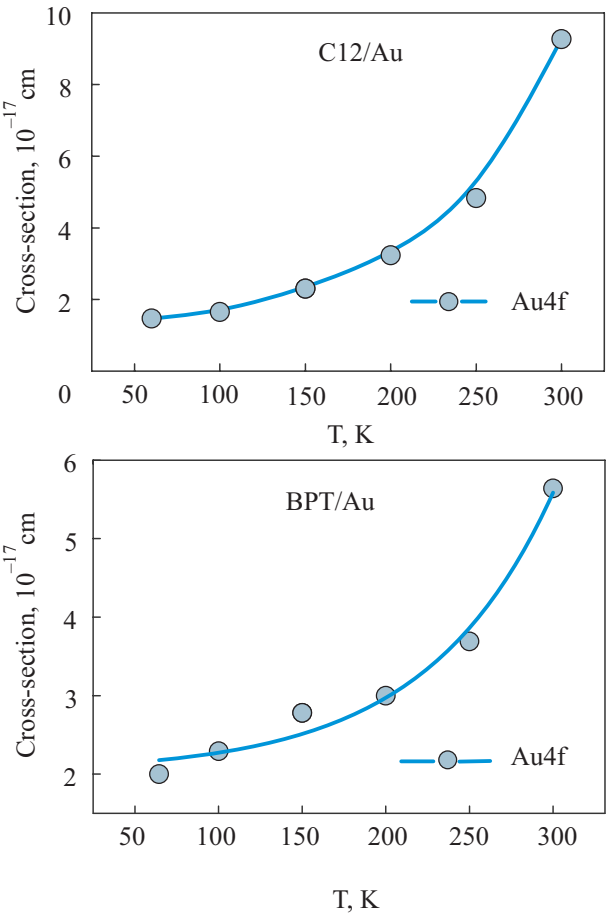

Fig. 4. Initial desorption cross-sections from (top) C12/Au ($h\nu = 250$ eV) and (bottom) BPT/Au ($h\nu = 310$ eV).

Irradiation induced material loss can also be monitored by x-ray photoelectron spectroscopy (XPS), e.g., by recording the film induced attenuation of the XPS signal from the substrate as a function of irradiation dose and film temperature. From such data cross-section values and information on the saturation behavior of beam damage can easily be derived. Figure 4 shows initial desorption cross-section values for thiolate bonded aliphatic (CH_3–$(CH_2)_{11}$–S–Au: C12/Au) and aromatic SAMs (C_6H_5–C_6H_4–S–Au: BPT/Au).

Integral PSD cross-sections (we continue using the term «PSD», although «ESD» contributes substantially, as shown above) are about $2 \cdot 10^{-17}$ cm^2 at 50 K, for C12/Au as well as for BPT/Au. Between 50 and 300 K they increase by a factor of 5 for C12/Au and 3 for BPT/Au. Both layers show saturation behavior, i.e., a dramatic reduction of beam effects for large exposures. This has previously been explained as due to cross-linking as a consequence of hydrogen abstraction. The cross linking network stabilizes the film against further radiation attack by hindering material transport. On the other hand, it enables horizontal delocalization of electronic excitations, thus reducing the probability of excitation localization at

an individual bond. This localization, however, is a prerequisite for the coupling of the electronic excitation to nuclear motion. At room temperature, this cross-linking effect is much more efficient for aromatic SAMs than for aliphatic layers, see Fig. 5, in perfect agreement with previous experiments [8].

We obviously encounter a competition between cross-linking and material loss. Cross-linking prevents further material loss, but rapid material loss makes the film so porous that cross-linking is hindered. From the above results we expect low temperatures to favor cross-linking compared with material loss, because cross-linking results from temperature independent hydrogen abstraction (Fig. 2), whereas material loss is enhanced by thermally stimulated diffusive transport (Figs. 3 and 4). The experimental results depicted in Fig. 5 agree with these expectations. The lower the temperature, the more efficient the cross-linking induced limitation of material loss. For aliphatic films with their large desorption cross-sections at room temperature (cf. Fig. 3) this effect is most pronounced and is of great practical importance. At room temperature stabilization by cross-linking is efficient *only* for aromatic SAMs, because for aliphatic SAMs material loss is *too fast* at that temperature. Under cryogenic conditions, however, aliphatic SAMs can be stabilized by radiation as well. Using temperature as a process parameter, compact and interconnected, or porous aliphatic films can easily be prepared by radiation. We believe this result to be of great importance for many applications, particularly for resist technology. Keeping in mind that cross-linking stabilizes not only against radiative but also against chemical attack, we foresee the process temperature as a tool to tailor negative or positive resist behavior from identical films.

Using thiolate bonded SAMs as an example, we finally focus on radiation induced modifications of the headgroup. In previous studies it has been shown that irradiation by electrons or photons breaks the thiolate bond, leading either to dialkylsulfide species if sulfur terminated hydrocarbon fragments diffuse from the substrate and get trapped by dangling bonds formed by hydrogen abstraction, or to accumulation of atomic sulfur at the substrate. Both species can be well discriminated in XPS. Film temperature modifies this branching (Fig. 6: C12/Au; results for BPT/Au are qualitatively similar).

The irradiation induced loss of thiolate species is clearly enhanced at 300 K; it is paralleled by the gain of the dialkylsulfide species. The build-up of atomic sulfur, a process in competition with the dialkylsulfide formation but of much smaller cross-section, is enhanced at low temperature, when the diffusive transport of larger fragments from the metal interface — a necessity for the dialkylsulfide formation — is hindered. We emphasize that negligible changes of the composition of the layer are obtained for heating *after* irradiation. This clearly indicates that cooling not simply *freezes* the structure, but *hinders permanent bond breaking* by preventing diffusive transport. This is a result of great importance in particular for cryospectroscopy: Cryogenic conditions may allow spectroscopic investigations of films which under room temperature suffer too rapid degradation. On the other hand, we can summarize that temperature is a parameter which steers electronically stimulated modification of all parts

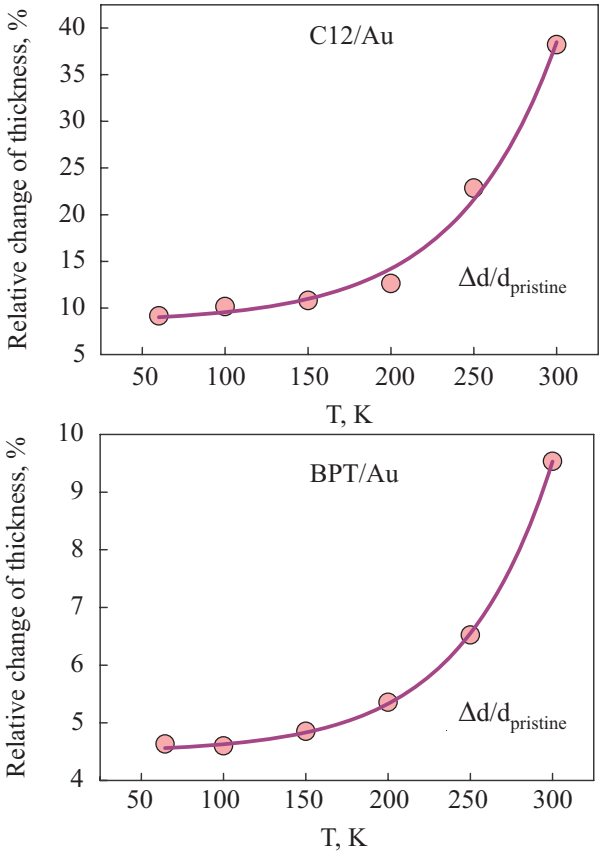

Fig. 5. Saturation behavior of beam damage as a function of temperature: Relative change of layer thickness after extended irradiation for C12/Au (top) and BPT/Au (bottom).

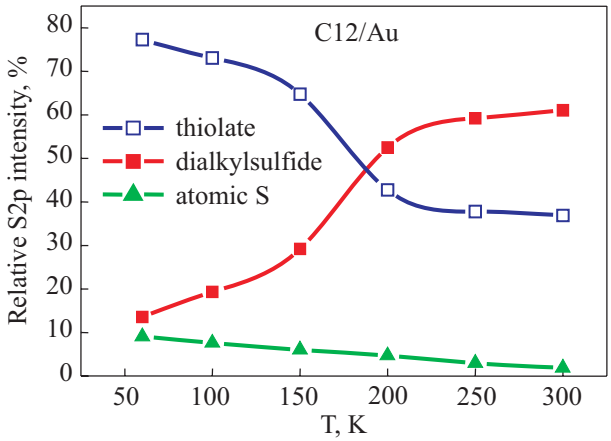

Fig. 6. Relative amounts of sulfur containing species after exposure to $5 \cdot 10^{16}$ $h\nu/cm^2$.

of thin organic films on surfaces, a result of the connection of thermal and electronic stimulation.

2.2. Beam induced conversion of water layers on Ru(001)

Products of beam induced modifications influencing thermally stimulated reactions is our next topic. Our example is chemisorbed water on the close-packed Ru(001) surface. Chemisorption of water is of interest for many fields ranging from electrochemistry over fuel cell technology to biological and medical applications. The chemisorption system H_2O/D_2O on Ru(001) is of special fundamental interest because it shows an uncommonly large isotope effect in thermal desorption (TD, Fig. 7).

Apart from multilayer contributions, TD of chemisorbed D_2O shows a single maximum for large as well as small heating rates. For H_2O, however, the TD spectrum is bimodal. The branching between low- and high-temperature TD maxima depends on the heating rate; the center of gravity is shifted to the second maximum for slow heating. The current interpretation of this unusual behavior based on DFT calculations, vibrational spectroscopy and low-energy electron diffraction (LEED) [19–22] is that the molecularly chemisorbed water layer corresponding to the low-temperature (= 1st) TD peak is a metastable state. It can transform into a more strongly bound partially dissociated layer corresponding to the high-temperature TD maximum which consists of H_2O + OH + H (D_2O + OD + D, see, e.g., Fig. 3 of [19]). This transformation is an activated process; the barrier between the molecularly chemisorbed and the partially dissociated state is for D_2O higher than the barrier for desorption; for H_2O it is lowered because of the larger zero point energy of the H–to–O vibration. As a result, two TD maxima are observed for H_2O, but only one for D_2O.

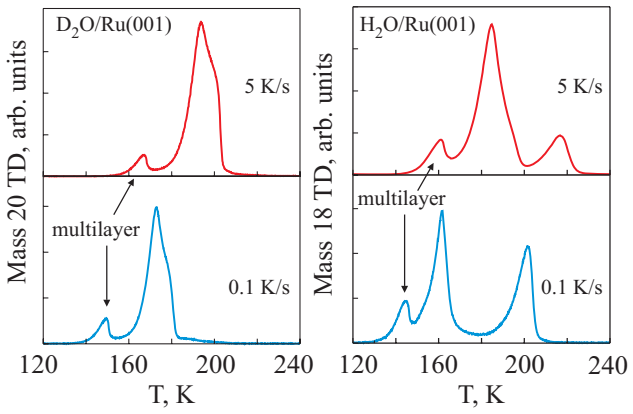

Fig. 7. TD spectra of D_2O (left) and H_2O (right) from chemisorbed layers on the Ru(001) surface as a function of the heating rate (after [17], in perfect agreement with [19]).

This subtle balance between two reaction pathways is efficiently disturbed by small amounts of co-adsorbates, e.g., oxygen or hydrogen atoms. Clay et al. [18] have shown that co-adsorbed oxygen in the percent range lowers the barrier between the molecular and partially dissociated state with respect to desorption, i.e., increases for H_2O the second TD maximum at the expense of the first one and induces for D_2O the second TD peak which does not exist for the pure layer. Only 0.09 monolayers (ML) of preadsorbed oxygen suffice for complete conversion in TD. Co-adsorbed hydrogen has the inverse effect. Clay's data are in qualitative agreement with previous results from Doering and Madey [23].

The assumptions about the geometry of the molecularly chemisorbed layer have experienced some evolution. The first investigations assumed a layer consisting of two types of differently oriented water molecules arranged in hexagons (Ref. 23, and references therein). Type I had its hydrogen atoms directed towards the O atoms of neighboring water molecules, whereas the hydrogen plane of type II was tilted by 90 degrees; one of the O–H bonds was directed to neighboring water, and the other one towards the vacuum («H-up», see, e.g., Figs. 13–15 in [23]). Essentially, this so-called bilayer was obtained by cutting one layer out of hexagonal bulk ice and putting it on a surface. In the meantime this picture has been modified, including also «H-down» molecules with one hydrogen directed towards the substrate, which probably is slightly more stable than H-up [19–22]. Very recently it has been proposed that arranging both above types (for type II exclusively H-down) in chains instead of hexagons could increase the binding energy even further [22].

The first studies of water on Ru(001) assumed exclusively molecular adsorption. The idea of partial dissociation was introduced by Feibelman in 2002 [24]. Based on DFT calculations he concluded that the chemisorption energy of a molecular layer would be lower than the condensation energy of bulk ice, i.e., the molecular layer would not wet the surface. As an alternative he suggested the existence of a more strongly bound partially dissociated layer consisting of H_2O + OH + H (D_2O + OD + D). In [24] a 1:1 ratio was proposed for the H_2O and H_2O + OH + H (D_2O, D_2O + OD + D) species, respectively. In a later publication this ratio had been changed to 5:3 in order to fit XPS results [25]. The low chemisorption energy of the molecular layer and the resulting «nonwetting» argument of [24,25] have been questioned on the basis of more refined DFT calculations and experiments (see, e.g., [22] and references therein). There is agreement now that for both H_2O and D_2O the pure layers before the start of desorption are molecular, i.e., water does wet the Ru surface. Agreement also exists, however,

that a partially dissociated water layer should be more stable than the molecular one (see above).

Feibelman's paper [24] prompted several theoretical as well as experimental studies on this systems. Two of them, both utilizing XPS with synchrotron radiation, came to fully opposite results [25,26]. Reference 25 reported XPS data indicating partial dissociation of H_2O and D_2O at 145 K from the beginning, whereas Ref. 26 found no dissociation of D_2O, minor dissociation for H_2O, and strong dissociation only for extended exposure to the synchrotron beam or for adsorption at elevated sample temperature, in agreement with the above TD results. In a study partly conducted in our lab we have shown that very low doses of secondary electrons can in fact cause rapid dissociation [17]. Due to experimental restrictions, it was not possible to irradiate the water layer homogeneously in this previous study, leading to some artifacts in the beam effect's saturation behavior. For the investigations presented here, we obtained a strictly homogeneous irradiation profile by scanning a small spot of 200 eV electrons rapidly over the surface by applying triangular voltages of different frequencies to the *x* and *y* deflection plates of the electron gun. Monitoring the sample current on an oscilloscope synchronously with the deflection allowed exact adjustment of the scan area to the sample size. From the scan area and the time integrated gun current we obtained electron exposures with an error of less than 10%.

Figure 8 shows TD spectra from chemisorbed D_2O layers after irradiation with 200 eV electrons under such conditions. These layers have been prepared by dosing D_2O beyond saturation of the chemisorbed layer, followed by controlled annealing to remove multilayer contributions before starting the electron bombardment (we will use the term «bilayer» for species obtained by this

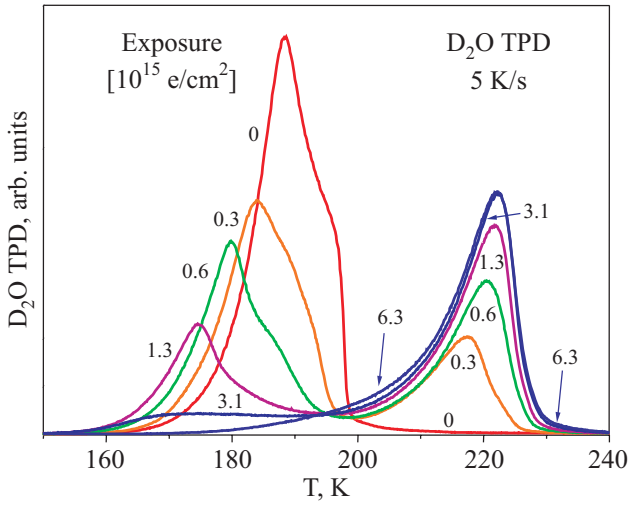

Fig. 8. Electron induced modifications of TD spectra from a saturated chemisorbed layer of D_2O/Ru(001) as a function of (homogeneously distributed) electron exposure.

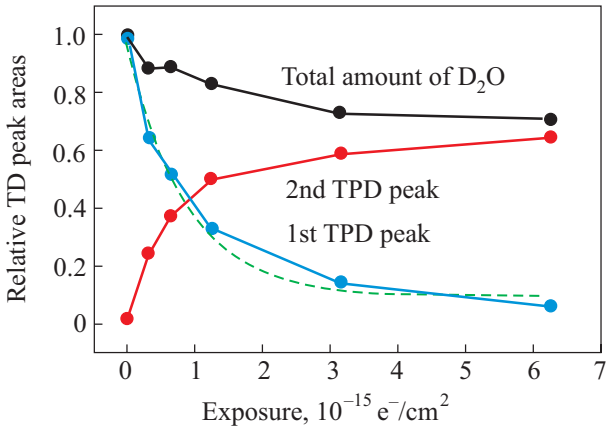

Fig. 9. TD peak areas as a function of electron exposure.

preparation procedure). After water desorption was completed, the samples were heated to 1570 K in order to remove all residual oxygen before preparing new bilayers. As observed previously [17], electron bombardment induces a second TD maximum at expense of the first. As noted previously, this second TD maximum was completely absent for the pristine D_2O bilayer. An electron dose of ~ $6 \cdot 10^{15}$ e/cm^2 sufficed for complete conversion (Fig. 9). This conversion is associated with a loss of ~30% of the total amount of D_2O (see TD data in Fig. 9). Fitting the decay of the first TD peak by a simple exponential we obtain a cross-section value of 10^{-15}cm^{-2} (dotted line in Fig. 9). This decay is due to conversion into the second TD maximum and to a lesser extent also to desorption, see Fig. 9.

The main differences of the present investigation compared with our previous study [17] is a larger conversion cross-section and the finding of complete conversion. The previously obtained saturation behavior of the conversion at large exposure obviously was due to an inhomogeneous irradiation profile.

The value for the conversion and desorption cross-section of 10^{-15}cm^{-2} is very large, even for dissociative electron attachment, a process which may exhibit large cross-section values. Considering the strong effect of co-adsorbed oxygen and hydrogen ([18] and above), we considered possible catalytic conversion activities of the reaction products produced by irradiation. If such activities were large, the apparent conversion cross-section would be a multiple of the cross-section of the primary electronically stimulated process. We checked this by dosing D_2O after thermal desorption of a previously irradiated layer *without* removing residues by flashing to 1570 K. Figure 10 shows the results. The TD results obtained after irradiation (full lines), and the TD spectra recorded after re-dosing of D_2O are practically identical, supporting the above hypothesis. We note that a qualitatively similar ef-

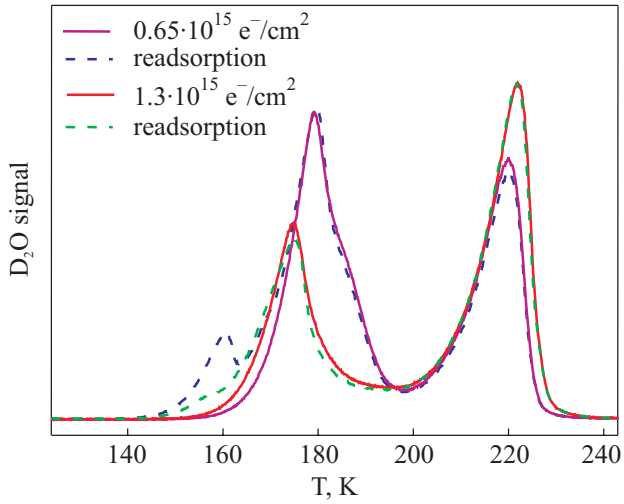

Fig. 10. TD spectra obtained after electron irradiation (full lines) and after readsorption of D_2O (broken lines). Readsorption was done by dosing an amount of D_2O corresponding to a full bilayer *after* the post-irradiation TD spectrum (full line) was completed. Because no annealing was applied in order not to disturb peak shapes, small multilayer contributions are visible at the leading edges of the readsorption spectra.

fect has been seen before already by Faradzhev [27] during the experiments reported in [17]. As will be shown below by XPS, irradiation induced perturbation of the hydrogen/oxygen balance catalyzes the conversion between the two TD states.

We note that electron bombardment beyond the dose necessary for complete conversion of the layer changes the shape of the TD peaks further (Fig. 11). Apart from an area reduction due to stimulated desorption of D_2O or D (both alternatives would reduce TD of intact water), we find additional shoulders at low as well as at high temperature. Similar effects have been observed for co-adsorption of large amounts of oxygen (cf. [23] and [28]).

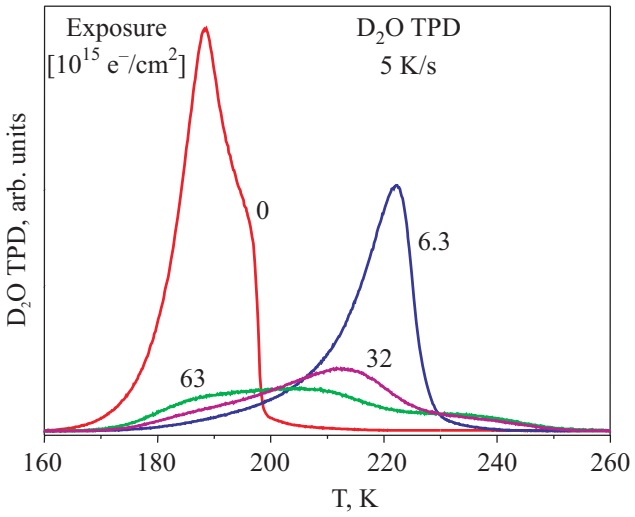

Fig. 11. TD spectra obtained after large homogeneous electron exposures.

O1s XPS data from D_2O bilayers after irradiation and after TD with a heating rate of 5 K/s up to 260 K are shown in Fig. 12. Care was taken to minimize beam damage. A small, constant, and preparation independent O1s contribution stemming from the crystal mount has been subtracted from all spectra. For pristine D_2O bilayers a single O1s maximum at 533 eV binding energy was observed in good agreement with [26] (the minimum exposure of $6\cdot10^{13}$ eV/cm^2 in Fig. 12 corresponds to that by Al K_α photons during data acquisition, i.e., its possible damage effect constitutes the minimum attainable). After TD of a pristine bilayer corresponding to zero exposure, no residual oxygen could be observed (Fig. 12). After irradiation of a D_2O bilayer with $6.3\cdot10^{15}$ e/cm^2, i.e., the dose which induces complete conversion, the O1s XPS peak became bimodal (Fig. 12). The main peak was shifted to a lower binding of 532.5 eV, and a second maximum appeared at 531 eV. The ratio of the two maxima was ~ 5:1.

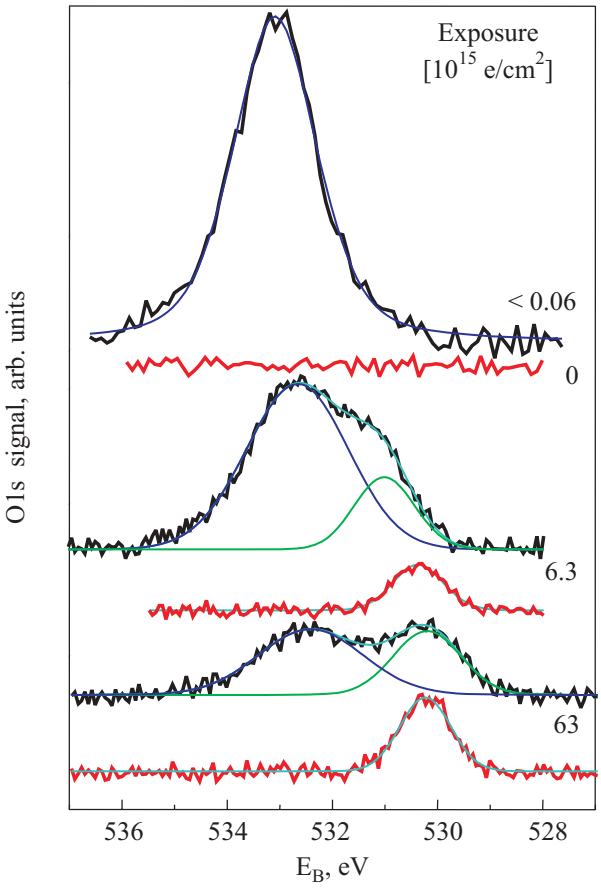

Fig. 12. XPS data for the O1s range obtained after electron irradiation (*a*), and after electron irradiation and TD up to 260 K (Al K_α radiation(*b*)); smooth lines are fitting results.

We note that the growth of the second O1s peak as well as the redshift of the first one occurred gradually with increasing electron exposure, without any threshold behavior. We also note that XPS spectra recorded from an initially completely converted layer *after* a TD run up to 200 K, i.e., the temperature corresponding to the minimum between the two TD peaks (Fig. 8), showed only marginal changes (not shown). The high beam effects (BE) maximum was slightly decreased due to TD in this temperature range (compare Fig. 8), and the low BE maximum was increased by ~10%, obviously due to conversion between the two states. Nevertheless, the ratio of both peak areas was still ~ 4:1.

This result is surprising with respect to the conversion of molecular to partially dissociated water sketched above [19–22]. Naively one would assign the first (i.e., low-temperature) TD peak to the molecularly absorbed layer, and the second one to the partially dissociated film. As a result, one would expect a single O1s peak corresponding to intact water for the pristine layer, and a two peak structure corresponding to the co-existence of $D(H)_2O$ and OD(H) + D(H) for the partially dissociated layer responsible for the second TD maximum. The one/two peak structures are observed, but the peak ratio at the onset of the second TD maximum fits neither the 1:1 ratio of the structure proposed in [24] nor the 5:3 ratio of the revised version from [25]. Area ratios close to 1:1 are observed *only* for electron exposures beyond the electron dose required for complete TD conversion (Fig. 12).

As mentioned above, no residual oxygen could be detected *after* TD of pristine D_2O layers. *After* TD of a layer irradiated until complete conversion ($6.3\cdot10^{15}$ e/cm^2 trace in Fig. 12), a residual oxygen signal at 530.5 eV BE corresponding to 8% of the initially present oxygen or ~ 0.1 ML was detected, in perfect agreement with the amount of *co-adsorbed* oxygen necessary for complete conversion [18]. Excessive bombardment increases the residual oxygen signal from 8 to 13% (Fig. 12). This value is close to the oxygen amount found in [25] *after* the desorption of nominally *pure* D_2O and H_2O layers.

From the results shown in Figs. 10 and 12 we conclude that irradiation with a distinct electron dose has the same effect on the TD spectrum and probably also on the composition of the layer as co-adsorption of exactly the amount of oxygen which is left over after TD of the irradiated layer. The XPS results, however, indicate that the irradiated layer is not simply a combination of D_2O, OD and isolated O; the O1s peak of low BE from the irradiated layer has a larger BE than the residual O obtained after TD. We obviously do not encounter isolated O atoms in the irradiated layer but O atoms which are always correlated with hydrogen. The binding energies for the post-TD O1s peak and for the OD_x peak of the irradiated layer become more equal for extended irradiation which also means increased loss of hydrogen (Fig. 12).

In summary, we conclude from our data that the beam effects observed in our study and previous ones are due to a beam induced perturbation of the H to O ratio in the adsorbed water layer, in perfect agreement with previous co-adsorption experiments [18]. Future experiments detecting selectively the amount of H on the surface during and after TD could test this hypothesis. This perturbation obviously has a very strong effect on the barrier for partial dissociation of the molecular layer which explains the very large effective conversion cross-section. Comparing TD (Fig. 9) and XPS results (Fig. 12 and text), we tentatively conclude that this beam (or co-adsorbate) induced partial dissociation is by far not complete at the minimum between the two TD peaks. According to our data only ~20% of the layer would be due to an OD like species. Further dissociation stabilizing the layer and leading to a continuously increasing activation energy for desorption is assumed to occur during TD of the second state. This would explain the shape of the high-temperature TD peak which because of recombinative desorption should show a reaction order not smaller than 1, but in fact exhibits a slope ratio of leading/trailing edges which is either typical for a reaction order < 1, or an activation energy which increases with decreasing coverage. As mentioned above, future in-situ analysis of the layer composition is required for final conclusions.

We finally would like to address the point of beam induced artifacts in previous studies. From the results above it is clear that layer modifications by irradiation cannot be discriminated from the effect of co-adsorbed oxygen; such oxygen could be due to incomplete removal of previously prepared layers or to poor vacuum. On the other hand, contamination by hydrogen would have the opposite effect. One could argue that the discrepancies between our present study and those of [17–22,26] compared with the results reported in [25] are due to hydrogen contamination in our case and in [17–22,26]. We believe this not to be the case. All our results have been obtained under very good UHV conditions (base pressure $2\cdot10^{-11}$mbar), and all results have been reproduced several times. In addition, perfect agreement exists between our study and those from Refs. 17–22, 26, where comparable.

In summary, chemisorption of water on the Ru(001) surface was found to be a challenging system for theorists as well as for experimentalists. For theoreticians because of the difficulties arising from treating hydrogen bonds correctly, and for experimentalists because of the extreme sensitivity of this system to perturbations by coadsorbates and by irradiation. On the other hand, this system is an outstanding example for the large effect which the products of a beam induced reaction can have on an intrinsi-

cally thermally stimulated process like the partial dissociation of the water molecule.

Acknowledgments

We thank D.L. Allara for supporting us with the substance for the nitrile terminated SAMs, K.L. Kostov, N. Faradzhev and T.E. Madey for helpful discussions, and M. Grunze for support of the SAM related experiments. Help during the experiments by K. Eberle, R. Schneider, and the staff of BESSY, in particular O. Schwarzkopf, H. Pfau, and W. Braun, is gratefully acknowledged. The investigations have been supported by the Deutsche Forschungsgemeinschaft (Fe 347/1-3), by the German BMBF (05 KS4VHA/4 and 05 ES3XBA/5), and by the German Fonds der Chemischen Industrie.

1. R.D. Levine, *Molecular Reaction Dynamics,* Cambridge University Press, Cambridge (2005).
2. One of these exceptions are reactions driven by hot electrons created by intense laser pulses; see, e.g., M. Brandbyge, P. Hedegård, T.F. Heinz, J.A. Misewich, and D.M. Newns, *Phys. Rev*. **B52**, 6042 (1995).
3. V.E. Cosslett, *J. Microscopy* **113**, 113 (1978); G. Schneider, in: *X-Ray Microscopy IV*, V.V. Aristov and A.I. Erko (eds.), Bogorodskii Pechatnik Publishing Company, Chernogolovka (1994), p. 181; G. Schneider, *Ultramicroscopy* **75**, 85 (1998); D. Weiß, G. Schneider, B. Niemann, P. Guttmann, R. Rudolf, and G. Schmahl, *Ultramicroscopy* **84**, 185 (2000).
4. A. Ulman, *Chem. Rev*. **96**, 1533 (1996); F. Schreiber, *Prog. Surf. Sci.* **65**, 151 (2000).
5. *Handbook of Nanotechnology*, B. Bushan (ed.), Springer, Berlin (2004).
6. A. Härtl, E. Schmich, J.A. Garrido, J. Hernando, S.C.R. Catharino, S. Walter, P. Feulner, A. Kromka, D. Steinmüller, and M. Stutzmann, *Nature Mater*. **3**, 736 (2004).
7. A. Gölzhäuser, W. Geyer, V. Stadler, W. Eck, M. Grunze, K. Edinger, Th. Weimann, and P. Hinze, *J. Vac. Sci. Technol*. **B18**, 3414 (2000) .
8. M. Zharnikov and M. Grunze, *J. Vac. Sci. Technol.* **B20**, 1793 (2002) and references therein.
9. M.A. Huels, P.-C. Dugal, and L. Sanche, *J. Chem. Phys.* **118**, 11168 (2003) and references therein.
10. E. Garand and P.A. Rowntree, *J. Phys. Chem*. **B109**, 12927 (2005) and references therein.
11. P. Feulner, T. Niedermayer, K. Eberle, R. Schneider, D. Menzel, A. Baumer, E. Schmich, A. Shaporenko, Y. Tai, and M. Zharnikov, *Phys. Rev. Lett.* **93,** 178302 (2004).
12. A. Shaporenko, M. Zharnikov, P. Feulner, and D. Menzel, *J. Phys. Condens. Matter* **18**, S1677 (2006) .
13. R. Romberg, S.P. Frigo, A. Ogurtsov, P. Feulner, and D. Menzel, *Surf. Sci.* **451**, 116 (2000).
14. E. Schmich, *Diploma Thesis*, Technische Universität München (2004).
15. S. Neppl, *Diploma Thesis*, Technische Universität München (2006).
16. S. Frey, A. Shaporenko, M. Zharnikov, P. Harder, and D. L. Allara, *J. Phys. Chem.* **B107**, 7716 (2003).
17. N. Faradzhev, K.L. Kostov, P. Feulner, T.E. Madey, and D. Menzel, *Chem. Phys. Lett*. **415**, 165 (2005).
18. C. Clay, S. Haq, and A. Hodgson, *Chem. Phys. Lett*. **388**, 89 (2004).
19. Sheng Meng, E.G. Wang, Ch. Frischkorn, M. Wolf, and Shiwu Gao, *Chem. Phys. Lett*. **402**, 384 (2005).
20. A. Michaelides, A. Alavi, and D.A. King, *J. Am. Chem. Soc.* **125**, 2746 (2003).
21. G. Materzanini, G.F. Tantardini, P.J.D. Lindan, and P. Saalfrank, *Phys. Rev.* **B71**, 155414 (2005).
22. S. Haq, C. Clay, G.R. Darling, G. Zimbitas, and A. Hodgson, *Phys. Rev*. **B73**, 115414 (2006).
23. D.L. Doering and T.E. Madey, *Surf. Sci*. **123**, 305 (1982).
24. P.J. Feibelman, *Science* **205**, 99 (2002).
25. J. Weissenrieder, A. Mikkelsen, J.N. Andersen, P.J. Feibelman, and G. Held, *Phys. Rev. Lett.* **93**, 196102 (2004).
26. K. Andersson, A. Nikitin, L.G.M. Pettersson, A. Nilsson, and H. Ogasawara, *Phys. Rev. Lett*. **93**, 196101 (2004).
27. N. Faradzhev (private communication).
28. M.J. Gladys, A. Mikkelsen, J.N. Andersen, and G. Held, *Chem. Phys. Lett.* **414**, 311 (2005).